

Interlocking Nailing Versus Interlocking Plating in Intra-articular Calcaneal Fractures: A Biomechanical Study

Foot & Ankle International®

1-7

© The Author(s) 2016

Reprints and permissions:

sagepub.com/journalsPermissions.nav

DOI: 10.1177/1071100716643586

fai.sagepub.com

Sophia Reinhardt, MD¹, Heiner Martin, PhD², Benjamin Ulmar, MD³,
Stefan Döbele, MD⁴, Hans Zwipp, MD⁵, Stefan Rammelt, MD⁵,
Martinus Richter, MD⁶, Martin Pompach, MD⁷, and Thomas Mittlmeier, MD¹

Abstract

Background: Open reduction and internal fixation with a plate is deemed to represent the gold standard of surgical treatment for displaced intra-articular calcaneal fractures. Standard plate fixation is usually placed through an extended lateral approach with high risk for wound complications. Minimally invasive techniques might avoid wound complications but provide limited construct stability. Therefore, 2 different types of locking nails were developed to allow for minimally invasive technique with sufficient stability. The aim of this study was to quantify primary stability of minimally invasive calcaneal interlocking nail systems in comparison to a variable-angle interlocking plate.

Material and Methods: After quantitative CT analysis, a standardized Sanders type IIB fracture model was created in 21 fresh-frozen cadavers. For osteosynthesis, 2 different interlocking nail systems (C-Nail; Medin, Nov. Město n. Moravě, Czech Republic; Calcanail; FH Orthopedics SAS; Heimsbrunn, France) as well as a polyaxial interlocking plate (Rimbus; Intercus GmbH; Rudolstadt, Germany) were used. Biomechanical testing consisted of a dynamic load sequence (preload 20 N, 1000 N up to 2500 N, stepwise increase of 100 N every 100 cycles, 0.5 mm/s) and a load to failure sequence (max. load 5000 N, 0.5 mm/s). Interfragmentary movement was detected via a 3-D optical measurement system. Boehler angle was measured after osteosynthesis and after failure occurred.

Results: No significant difference regarding load to failure, stiffness, Boehler angle, or interfragmentary motion was found between the different fixation systems. A significant difference was found with the dynamic failure testing sequence where 87.5% of the Calcanail implants failed in contrast to 14% of the C-Nail group ($P < .01$) and 66% of the Rimbus plate. The highest load to failure was observed for the C-Nail. Boehler angle showed physiologic range with all implants before and after the biomechanical tests.

Conclusion: Both minimally invasive interlocking nail systems displayed a high primary stability that was not inferior to an interlocking plate.

Clinical relevance: Based on our results, both interlocking nails appear to represent a viable option for treating displaced intra-articular calcaneal fractures.

Keywords: calcaneal fracture, minimally invasive fixation, biomechanical testing, stability, interlocking nail, locking plate

Introduction

Currently, open reduction and internal fixation is deemed to represent the gold standard for the surgical treatment of displaced intra-articular calcaneal fractures.^{2,16} Because of the complex anatomy and delicate soft-tissue envelope, the operative treatment is challenging.¹⁰ Furthermore, the frequently used extended lateral approach is associated with the risk for skin necrosis, infection, and delayed wound healing.^{4,15} Thus, minimally invasive techniques have been developed to minimize soft-tissue complications.^{9,16} Until now, most minimally invasive repair constructs have limited primary stability compared with the use of interlocking plates, which might represent a risk for secondary displacement, in particular, if the

patients start early active exercises and partial weight-bearing following reconstruction.^{5,10,11}

In this experimental study, the aim was to investigate the primary stability of current minimally invasive nail systems compared with a conventional variable-angle interlocking calcaneal plate. The null hypothesis was that the different interlocking nail systems and the interlocking plate would not differ in primary stability during the biomechanical test sequences.

Materials and Methods

Twenty-one fresh-frozen hindfoot cadavers (Medcure, Portland, OR) were used. The distribution of the calcaneal specimens was blinded and equal regarding gender (10

Table 1. Distribution of Calcaneal Specimens.

Specimen Number	Implant Group	Age (y)	Gender	Side	Ethnic Group	BMD (mg/cm ³)
1	Rimbus	62	Male	Right	Caucasian	238.8
6	Rimbus	61	Female	Left	Caucasian	173
9	Rimbus	59	Female	Left	Caucasian	187.4
11	Rimbus	63	Female	Right	Caucasian	164.9
12	Rimbus	53	Male	Left	Caucasian	65.43
18	Rimbus	61	Male	Left	Caucasian	81.8
3	Calcanail	61	Female	Right	Caucasian	171.9
4	Calcanail	63	Male	Left	Caucasian	157.9
5	Calcanail	55	Female	Right	Caucasian	67.1
13	Calcanail	63	Male	Right	Caucasian	209.3
15	Calcanail	61	Male	Right	Caucasian	195.5
16	Calcanail	57	Female	Right	Caucasian	188.8
17	Calcanail	56	Male	Left	Caucasian	200.1
21	Calcanail	55	Female	Left	Caucasian	110
2	C-Nail	64	Female	Left	Caucasian	90.5
7	C-Nail	59	Female	Right	Caucasian	203.9
8	C-Nail	62	Male	Left	Caucasian	151.1
10	C-Nail	59	Male	Right	Caucasian	121.2
14	C-Nail	61	Male	Left	Caucasian	177
19	C-Nail	55	Male	Right	Caucasian	170.7
20	C-Nail	42	Female	Left	Caucasian	185.6

female, 11 male specimens) and side (10 right-sided, 11 left-sided specimens; see Table 1).²¹ All specimens were kept frozen within 2 plastic bags at a temperature of -20°C .¹² Overnight, the specimens were thawed to room temperature.¹²

Prior to preparation, all specimens were scanned using CT-based densitometry (Aquilion 64; Toshiba Medical Systems Europe B.V., Zoetermeer, Netherlands), which additionally ensured that all specimens were free of bony pathology. After complete skin and soft-tissue removal, a Sanders IIb fracture model was created with the help of an oscillating saw.⁸ Therefore, in the sagittal plane the posterior facet was separated from the sustentaculum.⁸ It was followed by an osteotomy at the angle of Gissane to the first fracture line in the coronal plane.⁸ Afterwards, the posterior tuberosity was osteotomized in the coronal plane.⁸ Both osteotomies were performed at an angle of 45 degrees to the vertical plane to attain a subtalar wedge fragment. The last

fracture line was created horizontally in the transversal plane and separated the subtalar fragment from the central fragment. After reduction, the fragments were temporarily fixed with K-wires before definitive fixation.

For internal fixation, the following implants were used: (1) the interlocking C-Nail (Medin, Nové Město n. Moravě, Czech Republic), (2) the interlocking Calcanail (FH Orthopedics SAS, Heimsbrunn, France), and (3) the polyaxial interlocking Rimbus plate (Intercus GmbH Rudolstadt, Germany; Figures 1-3). The original plan to allocate an identical number of cadaver specimens and implants to each of the 3 experimental groups had to be changed because a single specimen randomized for the plate group was too small for fitting the plate. Therefore, for this size-reduced calcaneus, another fixation mode had to be chosen (Table 1). Reduction and fixation of the implants was evaluated with an image intensifier. In a previous study, the Rimbus plate was biomechanically superior in comparison

¹Department of Trauma, Rostock University Medical Center, Hand and Reconstructive Surgery, Rostock, Germany

²Department of Biomedical Engineering, Rostock University Medical Center, Rostock, Germany

³Department of Orthopaedics, University of Ulm, Ulm, Germany

⁴Department of Trauma and Reconstructive Surgery, University of Tübingen, Tübingen, Germany

⁵UniversitätsCentrum für Orthopädie und Unfallchirurgie, Universitätsklinikum "Carl Gustav Carus" der TU Dresden, Dresden, Germany

⁶Klinik für Fuß- und Sprunggelenkchirurgie, Nuremberg and Rummelsberg, Germany

⁷Department of Traumatology, Pardubice Regional Hospital, Pardubice, Czech Republic

Corresponding Author:

Sophia Reinhardt, MD, Rostock University Medical Center, Schillingallee 35, Rostock 18057, Germany.

Email: sophia.labs@gmx.de

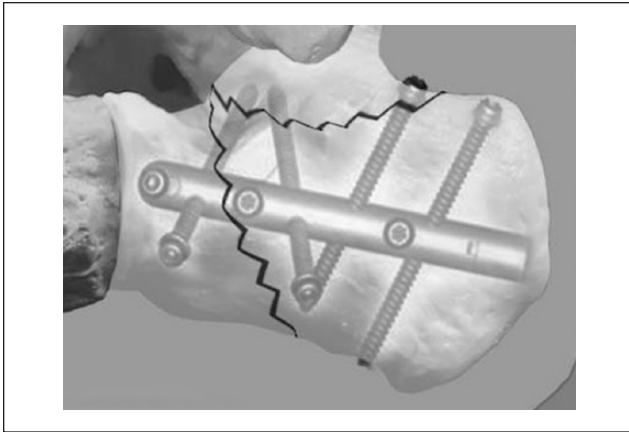


Figure 1. The C-Nail implant.



Figure 2. The Calcanail implant.

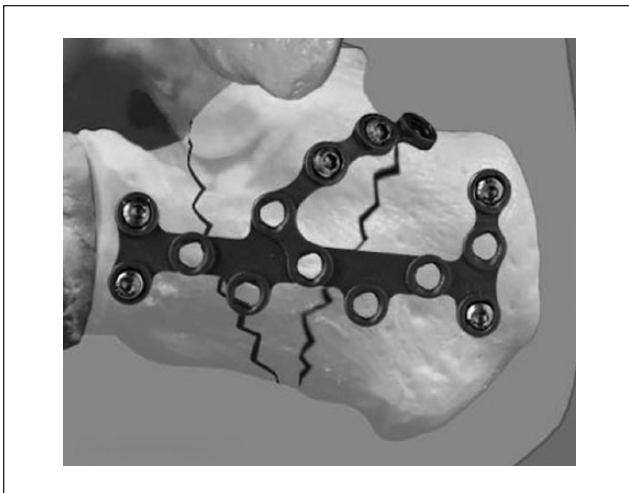


Figure 3. The Rimbus plate.

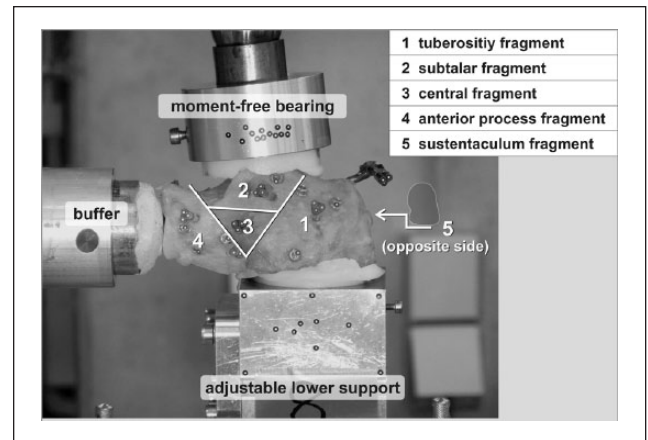


Figure 4. Fracture model and holding device mounted within the servohydraulic machine.

to other current interlocking plate designs.¹³ The placement of the screws in both interlocking nails with a differential thread allowed for angular stability when the screw head engages into the calcaneal cortex. All implants were inserted according to the manufacturer's recommendations. The plate was fixed with 6 screws in defined positions (anterior process, subtalar area, tuberosity). Furthermore, an additional subtalar screw was inserted in all specimens that were fixed with the interlocking nails.¹⁰

The specimens were embedded with the tuberosity fixed in veterinary polymethylmethacrylate (PMMA) bone cement (Demotec 95; Demotec Inc, Nidderau, Germany) within the testing device.^{13,14,21} An additional woodscrew was inserted into the posterior tuberosity in order to maximize the fixation strength of the bone cement. To ensure an anatomic hindfoot position, the holding device was adjusted individually in 3 planes.^{13,14,21} The anterior process was leaning against a buffer in the shape of the cuboid bone. Load was applied and transmitted through an individual PMMA cement-molded talus via a hydraulic testing machine (MTS, Eden Prairie, MN).^{13,14,21}

At least 3 markers were applied on each fragment (Figure 4). These markers were used in order to detect 3-dimensional interfragmentary motion by the optical measurement system (PONTOS 5M, GOM mbH, Braunschweig, Germany).¹ This measuring system was able to detect micromotion less than 5 μm and had successfully been used during previous biomechanical analyses.^{1,18} For interfragmentary motion analysis, the posterior tuberosity was set as local reference.

The same sequences were used as in a previous study.²¹ First, a dynamic cyclic loading was performed. This test started with a load of 1000 N and increased up to 2500 N with a stepwise load increment of 100 N after 100 cycles (preload 20 N; 1 Hz). If the constructs withstood this stress,

a load to failure sequence followed. Failure was defined by reaching the maximum load of 5000 N or a 0-degree gradient in the load deformation diagram.¹⁹ The load deformation data of the hydraulic testing device were registered via MTS FlexTest40 multipurpose testware software. Interfragmentary movement was detected by 2 charge-coupled device cameras connected to a computer.¹

Following osteosynthesis of all specimens and after the biomechanical tests, the Bohler angle was analyzed with fluoroscopy (Ziehm Vario 3D; Ziehm Imaging GmbH, Nuremberg, Germany). Bohler angle was defined as normal within the range of 20 to 40 degrees.⁷

Data are displayed as mean values \pm standard deviation. The statistical analysis was performed with 1-way analysis of variance (GraphPad Prism, version 6.0c; GraphPad Software, La Jolla, CA). When significant difference occurred in analysis of variance, a post hoc Tukey multiple comparison test was performed to locate the difference. In addition, Fisher exact test was used to analyze the number of failure events in the dynamic test sequence. The null hypothesis at a significance level of $P < .05$ was that there was no difference regarding the biomechanical performance of the 3 different implants.

Results

The bone mineral density of the specimens was essentially identical in all groups (Rimbus 151.9 ± 66.1 mg/cm³, C-Nail 157.1 ± 39.5 mg/cm³, Calcanail 162.6 ± 49.8 mg/cm³).

LTF was analyzed after the biomechanical tests. The maximum load of 5000 N was reached by one specimen with a C-Nail implant only. The C-Nail group had the highest load to failure, with a mean of 2808 (± 973.6) N. LTF with the Rimbus plate was 2041 (± 603.6) N and with the Calcanail 1751 (± 756.3) N (Figure 5). No significant difference in loads to failure between the groups could be found. Additionally, the number of failures in the dynamic test sequence was analyzed. In the dynamic testing sequence, 87.5% of the specimens treated with Calcanail, 66% of those fixed with the Rimbus plate and only 14% of the C-Nail group failed (Figure 6). The difference between the Calcanail and C-Nail groups was significant ($P = .01$; Fisher exact test). No significant difference could be found between the specimens fixed with the Rimbus plate fixation and any of the groups fixed with the interlocking nail systems.

Stiffness analysis during the dynamic testing sequence showed the highest stiffness in the Calcanail group (600.5 ± 451.6 N/mm) followed by Rimbus (532.8 ± 211.9 N/mm) and C-Nail (497.5 ± 171.6 N/mm). Because of the small amount of specimens that remained for the load to failure test (9/21), statistical analysis of the differences could not be performed.

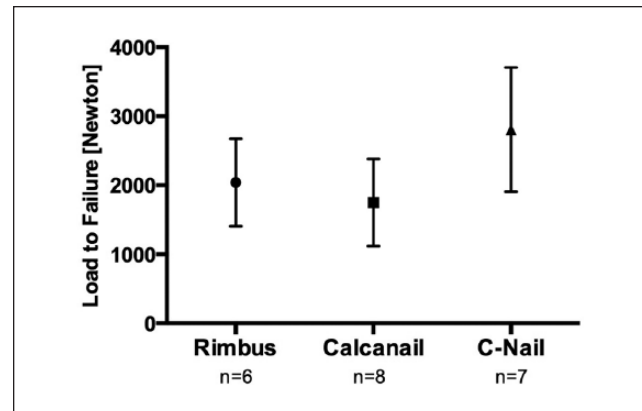


Figure 5. Load to failure (mean \pm 95% confidence interval).

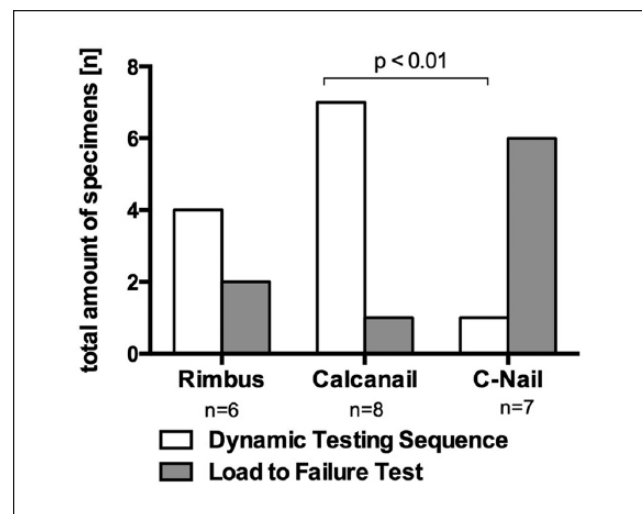


Figure 6. Failure in the dynamic testing sequence (n = absolute numbers).

Boehler angle was measured after osteosynthesis and after failure in any testing sequence. All implants showed a physiologic Bohler angle before and after biomechanical testing. The lowest decrease in Bohler angle could be detected in the Calcanail group (3.6 ± 3.0 degrees) after the biomechanical test whereas higher changes of Bohler angle could be seen in C-Nail specimens (8.0 ± 14.1 degrees) and Rimbus group (15.0 ± 6.1 degrees). None of these changes were statistically significant (Figure 7). Bone mineral density did not correlate with ultimate loads ($R^2 = 0.114$).

No significant differences with respect to interfragmentary motion during loading were detected between the 3 groups. The highest interfragmentary motion was detected in the anterior process fragment in the Calcanail and C-Nail groups. However, this was the only fragment where the

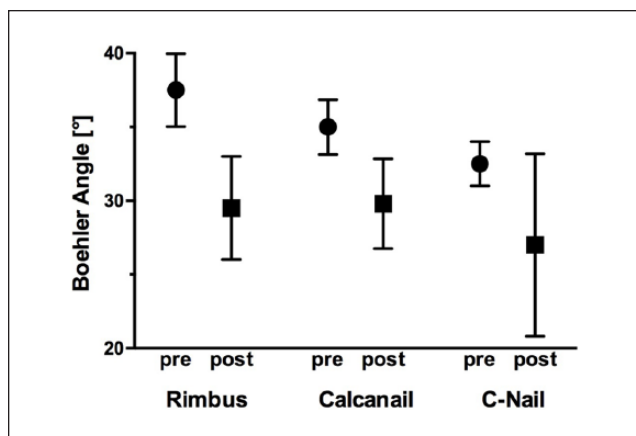


Figure 7. Boehler angle before and after the final biomechanical test (mean \pm 95% confidence interval).

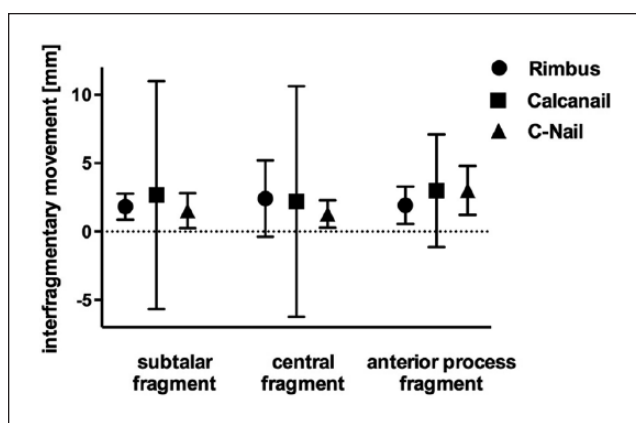


Figure 8. Interfragmentary motion of each fragment (mean \pm 95% confidence interval). Tuberosity and sustentacular fragment not shown.

Rimbus plate exhibited less mobility compared with both nailing systems. C-Nail had the least motion of the subtalar joint fragment and central fragments (Figure 8). None of the registered differences among the 3 groups were statistically significant.

Discussion

This biomechanical study compared 2 recently introduced interlocking nail systems with a variable-angle interlocking plate for internal fixation of displaced intra-articular calcaneal fractures with the aim to investigate the primary stability. Before biomechanical testing, any influence of variable bone mineral density was excluded because the specimens within the 3 experimental groups exhibited an identical bone mineral density.

Significant differences in load to failure could not be detected between the 3 groups. Interestingly, the maximum load of the protocol was reached only by one specimen belonging to the C-Nail group. During dynamic testing, the C-nail exhibited substantially fewer failures compared with the Calcanail. In comparison with the double interlocking mechanism of Calcanail, a higher degree of primary stability of the C-Nail was provided by 6 interlocking modes. Moreover, the sustentacular fragment was fixed with 2 of them. No correlation between bone mineral density and load to failure was seen. This indicates that the fixation techniques seemed to stabilize the fracture independently from the underlying bone quality as shown for implants at the distal fibula.²⁰ Goldzak et al compared the primary stability in a standardized fracture model employing the AO/ASIF calcaneal plate versus Calcanail and found substantially lower failure loads.⁴ This might be related to the dry enzymatically corroded cadaver bones they used.⁴ Another in vitro study had demonstrated increased load to failure values compared with our experiment.¹³ A different loading protocol in the dynamic test sequence and the use of sawbone specimens might be responsible for these different results.¹³ Sawbones exhibit a density that is 1.5 times higher than adult cadaver specimens. Based on comparative investigations, Sawbones were not recommended for further biomechanical investigations in the calcaneus.²¹ Differences in measured stiffness between nail and plate constructs had been confirmed by an earlier study, as well.⁴

A physiologic Boehler angle as a rough criterion for the reduction of the impacted subtalar surface and the restoration of outer calcaneal geometry may lead to a better outcome.^{4,6} Subtalar congruity is a recognized predictor of outcome after open reduction and internal fixation of intra-articular calcaneal fractures.¹¹ In our study, after completing biomechanical testing, the Boehler angle was within the physiologic range in all specimens. This result underscores the mechanical competency of all 3 tested implants to stabilize the fragment bearing the subtalar joint surface under the given high axial loading protocol. In addition, none of our specimens failed at the subtalar fragment, which is in accordance with the findings of Goldzak et al.⁴

Regarding interfragmentary motion differences observed between the 3 implants might be attributed to construct differences or inherent properties of the fracture model. The highest interfragmentary motion was detected in the central fragment in the Rimbus group. The central fragment was not addressed by the chosen screw arrangement of the experiment, whereas C-Nail and Calcanail showed the greatest relative motion at the anterior process fragment. With the Calcanail, the anterior process was not included with the fracture stabilization. Most important, the subtalar joint-bearing fragment exhibited least motion with all 3 implant types. As such, these results reflect implant-specific

differences, which had been described in part during earlier studies.^{4,13} In principle, adequate fixation of the fracture model was achieved with all 3 implant types.

This study has some limitations. The complete removal of all soft tissues in order to achieve adequate fixation in the testing jig led to an unphysiologic elimination of any soft tissue influences, for example, of the Achilles tendon.^{3,21} Furthermore, the study had been limited to a single fracture model. Creating fracture lines with an oscillating saw differs from the clinical fracture situation.^{8,15} In the study by Redfern et al, interfragmentary motion was detected on the lateral and medial aspects of the hindfoot, as well.¹² In our study, the motion analysis system measured the relative motion on only the lateral side of the calcaneus because a self-designed carbon pin construct for the detection of relative motion of the sustentacular fragment failed. In addition, the local reference for the interfragmentary motion had been defined in the tuberosity. Therefore, just 3 of the 5 fracture fragments could be traced independently.

Conclusion

In this study, we found that the primary stability of calcaneal interlocking nail systems tested in a standardized cadaver fracture model was not inferior to an interlocking plate that itself had been proven to provide a high degree of primary stability compared with other current plate designs.^{13,14} In a clinical setting, both interlocking nails could be used with a minimally invasive technique. Therefore, clinical implementation of calcaneal interlocking nails has the potential to compensate for the drawbacks of most minimally invasive stabilization techniques (eg, K-wires, isolated screws, small-sized plates) that have a rather limited primary mechanical stability.^{11,17} Both calcaneal interlocking nail options appear to represent a viable option for the treatment of displaced intra-articular calcaneal fractures and may allow for early active exercises and partial weight-bearing without the inherent risk of secondary displacement. Recently published clinical experiences with the C-Nail and Calcaneal support these data with a favorable clinical outcome.^{17,22}

Acknowledgments

The authors want to thank Thomas Wodetzki, Rostock, for the graphical work. Furthermore, the authors are grateful to Gerhard Scharr, Institute of Mechanical Engineering and Ship Building Technology, Rostock University, and Sebastian Gühring, University of Tübingen, Dept. of Trauma and Reconstructive Surgery, who helped with the test setup.

Declaration of Conflicting Interests

The author(s) disclosed the following potential conflicts of interest with respect to the research, authorship, and/or publication of

this article: Hans Zwipp, MD, reports personal fees, during the conduct of the study; In addition, he has a patent 300464 calcaneal nail with royalties paid. Stefan Rammelt, MD, reports that he is a member of the AO Foot & Ankle Expert Group and AO Foot & Ankle Education Taskforce. He has received travel support from AO Trauma and DePuy Synthes. Thomas Mittlmeier, MD, reports a patent Clou d'osteosynthese du calcaneum Fr no. 10/59724 issued. Martinus Richter, MD, reports a patent Rimbus plate system with royalties paid and a consultant for Curvebeam, Stryker, Intercus, Ulrich, proprietor of R-Innovation, and joint proprietor of First Worldwide Orthopaedic. Martin Pompach, MD, reports personal fees from MEDIN, during the conduct of the study; in addition, he has a patent 300464 calcaneal nail with royalties paid.

Funding

The author(s) received no financial support for the research, authorship, and/or publication of this article.

References

1. Doebele S, Siebenlist S, Vester H, et al. New method for detection of complex 3D fracture motion—verification of an optical motion analysis system for biomechanical studies. *BMC Musculoskelet Disord*. 2012;13(9):13-33. <http://dx.doi.org/10.1186/1471-2474-13-33>.
2. Epstein N, Chandran S, Chou L. Current concepts review: intra-articular fractures of the calcaneus. *Foot Ankle Int*. 2012;33(1):79-86. <http://dx.doi.org/10.3113/FAI.2012.0079>.
3. Essex-Lopresti P. The mechanism, reduction technique, and results in fractures of the os calcis. *Br J Surg*. 1952;39(3):395-419.
4. Goldzak M, Simon P, Mittlmeier T, Chaussemier M, Chiergatti R. Primary stability of an intramedullary calcaneal nail and an angular stable calcaneal plate in a biomechanical testing model of intraarticular calcaneal fracture. *Injury*. 2014;45(1):49-53. <http://dx.doi.org/10.1016/j.injury.2013.10.031>.
5. Illert T, Rammelt S, Drewes T, Grass R, Zwipp H. Stability of locking and non-locking plates in an osteoporotic calcaneal fracture model. *Foot Ankle Int*. 2011;32(3):307-313. <http://dx.doi.org/10.3113/FAI.2011.0307>.
6. Janzen DL, Connell DG, Munk PL, et al. Intraarticular fractures of the calcaneus: value of CT findings in determining prognosis. *AJR Am J Roentgenol*. 1992;158(6):1271-1274. <http://dx.doi.org/10.2214/ajr.158.6.1590122>.
7. Knight JR, Gross EA, Bradley GH, Bay C, LoVecchio F. Bohler's angle and the critical angle of Gissane are of limited use in diagnosing calcaneus fractures in the ED. *Am J Emerg Med*. 2006;24(4):423-427. <http://dx.doi.org/10.1016/j.ajem.2005.12.013>.
8. Lin PP, Roe S, Kay M, Abrams CF, Jones A. Placement of screws in the sustentaculum tali. A calcaneal fracture model. *Clin Orthop Relat Res*. 1998;352(6):194-201.
9. Nelson JD, McIff TE, Moodie PG, Iverson JL, Horton GA. Biomechanical stability of intramedullary technique for fixation of joint depressed calcaneus fracture. *Foot Ankle Int*. 2010;31(3):229-235. <http://dx.doi.org/10.3113/FAI.2010.0229>.

10. Rammelt S, Zwipp H. Calcaneus fractures: facts, controversies and recent developments. *Injury*. 2004;35(5):443-461. <http://dx.doi.org/10.1016/j.injury.2003.10.006>.
11. Rammelt S, Zwipp H. Fractures of the calcaneus: current treatment strategies. *Acta Chir Orthop Traumatol Cech*. 2014;81(3):177-196.
12. Redfern DJ, Oliveira MLR, Campbell JT, Belkoff SM. A biomechanical comparison of locking and nonlocking plates for the fixation of calcaneal fractures. *Foot Ankle Int*. 2006;27(3):196-201.
13. Richter M, Droste P, Goesling T, Zech S, Krettek C. Polyaxially-locked plate screws increase stability of fracture fixation in an experimental model of calcaneal fracture. *J Bone Joint Surg Br*. 2006;88(9):1257-1263. <http://dx.doi.org/10.1302/0301-620X.88B9.17822>.
14. Richter M, Gosling T, Zech S, et al. A comparison of plates with and without locking screws in a calcaneal fracture model. *Foot Ankle Int*. 2005;26(4):309-319. <http://dx.doi.org/10.1177/107110070502600407>.
15. Sanders R. Displaced intra-articular fractures of the calcaneus. *J Bone Joint Surg Am*. 2000;82(2):225-250.
16. Schepers T. The sinus tarsi approach in displaced intra-articular calcaneal fractures: a systematic review. *Int Orthop*. 2011;35(5):697-703. <http://dx.doi.org/10.1007/s00264-011-1223-9>.
17. Simon P, Goldzak M, Eschler A, Mittlmeier T. Reduction and internal fixation of displaced intra-articular calcaneal fractures with a locking nail: a prospective study of sixty nine cases. *Int Orthop*. 2015;39(10):2061-2067. <http://dx.doi.org/10.1007/s00264-015-2816-5>.
18. Steiner T, Raith S, Eichhorn S, et al. Evaluation of a new optical measuring system for experiments on fractured human mandibles: a biomechanical feasibility study in maxillofacial surgery. *Clin Oral Investig*. 2012;16(6):1535-1542. <http://dx.doi.org/10.1007/s00784-011-0659-z>.
19. Stoffel K, Booth G, Rohrl SM, Kuster M. A comparison of conventional versus locking plates in intraarticular calcaneus fractures: a biomechanical study in human cadavers. *Clin Biomech*. 2007;22(1):100-105. <http://dx.doi.org/10.1016/j.clinbiomech.2006.07.008>.
20. Zahn RK, Frey S, Jakubietz RG, et al. A contoured locking plate for distal fibular fractures in osteoporotic bone: a biomechanical cadaver study. *Injury*. 2012;43(6):718-725. <http://dx.doi.org/10.1016/j.injury.2011.07.009>.
21. Zech S, Goesling T, Hankemeier S, et al. Differences in the mechanical properties of calcaneal artificial specimens, fresh frozen specimens, and embalmed specimens in experimental testing. *Foot Ankle Int*. 2006;27(12):1126-1136. <http://dx.doi.org/10.1177/107110070602701220>.
22. Zwipp H, Rammelt S, Amlang M, Pompach M, Dürr C. Operative treatment of displaced intra-articular calcaneal fractures. *Oper Orthop Traumatol*. 2013;25(12):554-568. <http://dx.doi.org/10.1007/s00064-013-0246-3>.